

steepness of the refractive index profile is maintained at the same value throughout the stack. Thick stacks of a constant small slope are equivalent to thin stacks of a constant large slope. This greatly eases the requirements for close control of the growth process.

ACKNOWLEDGMENTS

Much of this work is based on a group effort. We acknowledge contributions by G. E. Carver, H. S. Gurev, R. E. Hahn, K. D. Masterson, and K. P. Murphy. Special recognition is due to James Rancourt for his help with the computational part of this paper. Our program is supported by the U.S. Energy Research and Development Agency under Contract No. E(29-2)-3709.

*Visiting Professor with permanent address at Laboratoire de Spectroscopie II, Université des Sciences et Techniques du Languedoc, Place Eugène Bataillon 34060 Montpellier, France.

¹H. Tabor, in *Transactions of the Conference on the Use of Solar Energy* (1955), Vol. 2, Part I, Sec. A, p. 32.

²J. T. Gier and R. V. Dunkle, in *Transactions of the Conference on the Use of Solar Energy* (1955), Vol. 2, Part I, Sec. A, p. 41.

³B. O. Seraphin and A. B. Meinel, in *Optical Properties of Solids—New Developments*, edited by B. O. Seraphin (North-Holland,

Amsterdam, 1975), Chap. 17, p. 927.

⁴V. A. Wells, B. O. Seraphin, and L. S. Raymond, in *Proceedings of the 4th International Conference on Chemical Vapor Deposition* (Electrochemical Society, New York, 1973) p. 512.

⁵R. E. Hahn and B. O. Seraphin, "Thick semiconductor films for photothermal solar energy conversion," *J. Vac. Sci. Technol.* **12**, 905 (1975).

⁶B. O. Seraphin, "Chemical vapor deposition of thin semiconductor films for solar energy conversion," *Thin Solid Films* **39**, 87 (1976).

⁷H. S. Gurev, G. E. Carver, and B. O. Seraphin, *Solar Energy* (Electrochemical Society, New York, 1976), p. 36.

⁸*American Institute of Physics Handbook*, 1972 edition, Chap. 6, p. 135-150; H. R. Philipp and A. Taft, *Phys. Rev.* **120**, 37-38 (1960); C. D. Salzberg and J. J. Villa, *J. Opt. Soc. Am.* **47**, 244-246 (1957); P. A. Schumann, Jr *et al.*, *J. Electrochem. Soc.* **118**, 45-148 (1971).

⁹J. T. Cox, and G. Mass, *Physics of Thin Films*, Vol. 2 (Academic, New York, 1963).

¹⁰W. Heitmann, "Reactive evaporation in ionized gases," *Appl. Opt.* **10**, 2414 (1971); "Properties of evaporated SiO₂, SiO_xN_y, and TiO₂ films," *Appl. Opt.* **10**, 2685 (1971).

¹¹Extraterrestrial spectral distribution of the solar flux $I_S(\lambda)$ is used in the calculation.

¹²J. Ritter, *Opt. Acta* **9**, 197 (1962).

¹³M. J. Rand, and J. F. Roberts, *J. Electrochem. Soc.*, **120**, 446 (1973).

¹⁴I. T. Ritchie, and W. Window, "Applications of thin graded-index films to solar absorbers," *Appl. Opt.* **16**, 1438 (1977).

Modes of optical waveguides

Allan W. Snyder

Institute of Advanced Studies, Departments of Applied Mathematics and Neurobiology, Australian National University, Canberra, Australia

William R. Young

Institute of Advanced Studies, Department of Applied Mathematics, Australian National University, Canberra, Australia
(Received 6 September 1977)

A simple method is presented for finding the modes on those optical waveguides with a cladding refractive index that differs only slightly from the refractive index of the core. The method applies to waveguides of arbitrary refractive index profile, arbitrary number of propagating modes, and arbitrary cross section. The resulting modal fields and their propagation constants display the polarization properties of the waveguide contained within the $\nabla \cdot \epsilon$ term of the vector wave equation. Examples include modes on waveguides with circular symmetry and waveguides with two preferred axes of symmetry, e.g., an elliptical core. Only a minute amount of eccentricity is necessary for the well-known LP modes to be stable on an elliptical core, while the circle modes couple power among themselves.

I. INTRODUCTION

We present a simple method for determining the modes of an optical waveguide with a cladding refractive index n_{cl} that differs only slightly from the maximum refractive index of the core n_{co} . The analysis does not require the waveguide to be multimoded or the refractive index profile to vary "slowly." Our procedure, called the $n_{co} \cong n_{cl}$ method, applies to waveguides of arbitrary cross section and arbitrary profile grading. It is a direct generalization of the $n_{co} \cong n_{cl}$ approximation¹ for modes of the step profile, circularly symmetric waveguide and provides results consistent with the generalized properties of graded profiles previously reported.²⁻⁴

The $n_{co} \cong n_{cl}$ method synthesizes the vector modal fields from linear combinations of solutions to the scalar wave equation. The appropriate linear combinations are dictated by properties of the $\nabla \cdot \epsilon$ terms in the vector wave equation. Failure to account for the $\nabla \cdot \epsilon$ terms, however small, will in general lead to "pseudo-modes" with the property that their cross sectional intensity and polarization pattern changes as the mode propagates.^{5,6} The LP modes⁵ of circularly symmetric waveguides are an example of pseudo-modes.

We briefly review several fundamental concepts required for the paper: when the permittivity $\epsilon(x,y)$ of the medium has cylindrical (not necessarily circular) symmetry, e.g. see Fig. 1, the modal electric \mathbf{E} and magnetic \mathbf{H} vector fields have

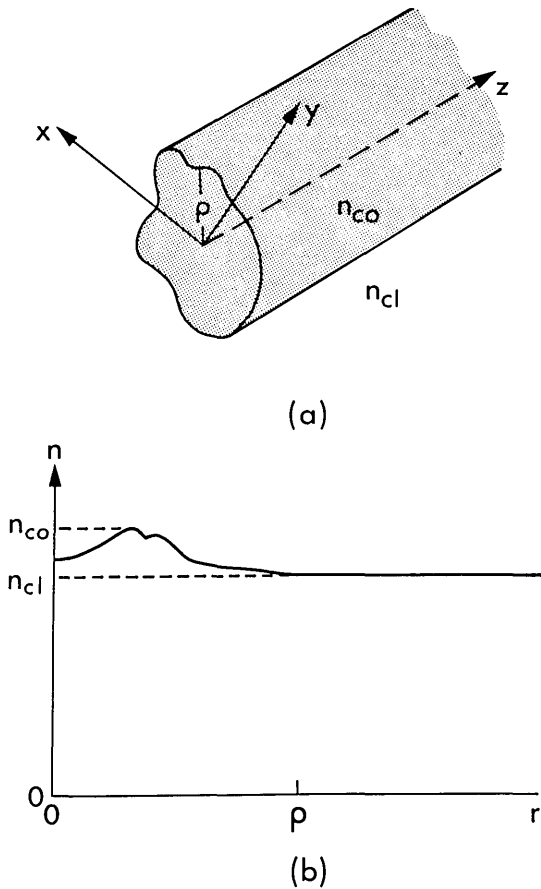


FIG. 1. (a) A waveguide with cylindrical symmetry. (b) The refractive index profile in some arbitrary cross section.

the form

$$\mathbf{E}(x,y,z) = \mathbf{e}(x,y)e^{i\beta z} = (\mathbf{e}_t + \mathbf{e}_z)e^{i\beta z}, \quad (1a)$$

$$\mathbf{H}(x,y,z) = \mathbf{h}(x,y)e^{i\beta z} = (\mathbf{h}_t + \mathbf{h}_z)e^{i\beta z}, \quad (1b)$$

assuming an $e^{-i\omega t}$ time dependence. The fields \mathbf{e}_t are solutions of the reduced wave equation

$$\nabla_t^2 \mathbf{e}_t + (k^2 - \beta^2)\mathbf{e}_t = -\nabla_t(\mathbf{e}_t \cdot \nabla_t \ln \epsilon), \quad (2)$$

where

$$\nabla_t = \nabla - \hat{z}(\partial/\partial z), \quad (3)$$

∇^2 is the transverse vector Laplacian,⁷ \hat{z} is a unit vector in the axial direction,

$$k(x,y) = \omega[\mu\epsilon(x,y)]^{1/2} = 2\pi n(x,y)/\lambda, \quad (4)$$

$\epsilon = \epsilon_0 n^2$ and ϵ_0 is the permittivity of free space. The remaining field components are determined from \mathbf{e}_t using Maxwell's equations. The allowed values of β result by demanding only that solutions of Eq. (2) be bounded, since effects of any discontinuities in ϵ are fully contained within the $\nabla_t(\ln \epsilon)$ term. For bound modes β is real and restricted to the range^{8,9}

$$k_{cl} \leq \beta \leq k_{co}, \quad (5)$$

where $k_{cl} = 2\pi n_{cl}/\lambda$, $k_{co} = 2\pi n_{co}/\lambda$, n_{co} is the maximum refractive index of the core, and n_{cl} is the refractive index of the cladding. Because of the $\nabla_t \ln \epsilon$ terms in the vector wave

equation, the modal fields are in general hybrid, possessing both e_z and h_z components. Furthermore, the bound modes of a lossless structure can always⁹ be written with \mathbf{e}_t , \mathbf{h}_t real and \mathbf{e}_z , \mathbf{h}_z imaginary.

II. THE $n_{co} \cong n_{cl}$ METHOD FOR DERIVING MODES: MOTIVATION

In this section we derive approximations for modal fields and their propagation constants on waveguides with $n_{co} \cong n_{cl}$ (see Fig. 1). The motivation¹ for our approximation begins by noting that the fields of optical waveguides can be expressed in terms of three parameters: The first is the complement of the critical angle θ_c , where

$$\sin \theta_c = \{1 - n_{cl}^2/n_{co}^2\}^{1/2} \simeq \theta_c. \quad (6)$$

The second parameter is the well-known dimensionless waveguide parameter V where

$$V = \rho\{k_{co}^2 - k_{cl}^2\}^{1/2} = k_{co}\rho \sin \theta_c, \quad (7)$$

ρ is one, of perhaps many, characteristic dimensions of the waveguide cross section, e.g., the core radius for circularly symmetric waveguides, $k_{co} = 2\pi n_{co}/\lambda$.

The third parameter describes the cross sectional geometry and the refractive index profile of the core; however, given θ_c and V , this parameter is redundant for the step refractive index waveguide of either planer or circular geometry. We make no explicit reference to this last parameter in our present analysis because it is not a function of θ_c .

When $\theta_c \ll 1$, the fields of optical waveguides can be expanded as a power series in θ_c , treating V and θ_c as independent variables,¹ e.g.,

$$\mathbf{e}(V, \theta_c) = \mathbf{e}_0(V, 0) + \theta_c \mathbf{e}_1(V, 0) + \theta_c^2 \mathbf{e}_2(V, 0) \dots$$

It is found that $\mathbf{e}(V, 0)$ is an excellent approximation to $\mathbf{e}(V, \theta_c)$, i.e., the fields have only a weak explicit dependence on θ_c . We emphasize that V is arbitrary even though $n_{co} = n_{cl}$. It is interesting that a waveguide with $n_{co} = n_{cl}$ and specific cross sectional core dimensions is unphysical because the wavelength λ of the exciting source must be zero in order to have V arbitrary. Furthermore, as a consequence of $\lambda = 0$, Eq. (5) shows that the modal propagation constant β is infinite. Thus, the fields of the $n_{co} = n_{cl}$ waveguide, although unphysical, nevertheless provide an excellent approximation to the physical $n_{co} \simeq n_{cl}$ waveguide. This paper is based on this last fact. Incidentally, the $n_{co} = n_{cl}$ approximation is analogous to the point dipole approximation of physical dipoles.¹⁰

Our purpose is to develop a direct method for finding expression for the $n_{co} \simeq n_{cl}$ waveguide because exact expressions are known for a few special cases only and even in these special cases the expressions tend to be algebraically complex compared to the $n_{co} \simeq n_{cl}$ forms. One method of derivation is to use standard perturbation techniques on Eq. (2), expanding $\mathbf{e}(V, \theta_c)$ in powers of θ_c ; however, we prefer to use a more physical approach starting with an intuitive derivation of the $n_{co} = n_{cl}$ waveguide.

A. The $n_{co} = n_{cl}$ waveguide

We begin by finding the modes of optical waveguides in the

artificial limit when the maximum refractive index of the core equals that of the cladding refractive index, i.e., when

$$n_{co} = n_{cl}. \quad (8)$$

By itself, this condition would appear to assume that the medium is homogeneous and incapable of guiding energy. However, to avoid the trivial consequences of this unintended assumption, we impose the crucial constraint¹ that the guiding properties of the structure remain unchanged, i.e., that the waveguide parameter V of Eq. (7) be an arbitrary constant. We next investigate the properties of modes on an $n_{co} = n_{cl}$ waveguide.

B. TEM modes of the $n_{co} = n_{cl}$ waveguide (LP modes)

Because bound modes are restricted to the range of values in Eq. (5), the limit $n_{co} = n_{cl} = n$ demands that

$$\beta = k_{co} = k_{cl} = k = 2\pi n/\lambda. \quad (9)$$

This condition is satisfied only by a z -directed transverse electromagnetic (TEM) wave, i.e., by a wave for which the electric and magnetic field vectors lie in a plane that is transverse to the axis of the waveguide. Accordingly, the modal fields of the $n_{co} = n_{cl}$ waveguide are

$$\tilde{\mathbf{h}}_z = \tilde{\mathbf{e}}_z = 0, \quad (10)$$

$$\tilde{\mathbf{h}}_t = (\epsilon/\mu)^{1/2} \hat{\mathbf{z}} \times \tilde{\mathbf{e}}_t, \quad (11)$$

where μ is the magnetic permeability of the media and a \sim is used to indicate quantities shown below to be associated with the scalar wave equation.

Because $n_{co} = n_{cl}$, all polarization-dependent properties of the structure are removed. If this is not obvious, then recall that as $n_{co} \rightarrow n_{cl}$, TE and TM waves undergo identical reflection at an interface between two semi-infinite media or at a caustic.^{9,11} Since the $\nabla_t \ln \epsilon$ term in the vector wave equation Eq. (2) is solely responsible for the polarization properties of modes, it is omitted solving for the $\tilde{\mathbf{e}}$ fields of the $n_{co} = n_{cl}$ waveguide. In other words, the fields of the $n_{co} = n_{cl}$ waveguide are solutions to the scalar wave equation. These vector modal fields can then be expressed in rectangular coordinates as

$$\tilde{\mathbf{e}}_x = \psi \hat{\mathbf{x}}, \quad \tilde{\mathbf{e}}_y = \psi \hat{\mathbf{y}}, \quad (12)$$

where $\hat{\mathbf{x}}$ and $\hat{\mathbf{y}}$ are unit vectors, ψ is a solution to

$$\{\nabla_t^2 + k^2 - \tilde{\beta}^2\}\psi = 0, \quad (13)$$

and ∇_t^2 is the transverse portion of the scalar Laplacian operator. The solutions ψ must be bounded everywhere and have the well-known property of the scalar wave equation that ψ and its normal derivative are everywhere continuous. These constraints lead to an eigenvalue equation from which the allowed values of $\tilde{\beta}$ are found, where $\tilde{\beta}$ is distinguished from β by being an eigenvalue of Eq. (13) rather than Eq. (2).

This completes our discussion of the $n_{co} = n_{cl}$ waveguide. Before continuing our development, we first anticipate possible misunderstanding. The $n_{co} = n_{cl}$ waveguide is unphysical because $\lambda = 0$ and hence $\beta = \infty$ in order for V to be arbitrary. Nevertheless, as we show later, the fields of the $n_{co} = n_{cl}$ waveguide are the building blocks for the $n_{co} \simeq n_{cl}$ waveguide. The $n_{co} = n_{cl}$ waveguide is, in general, unrelated to a multimoded ($V \gg 1$) waveguide so that geometrical or

asymptotic methods are not applicable. The values of $\tilde{\beta}$ determined from Eq. (13) are shown later to include the first-order effects of finite θ_c , even though $\tilde{\beta} \rightarrow k \rightarrow \infty$ as $n_{co} \rightarrow n_{cl}$. Because $\tilde{\beta} = k$ when $n_{co} = n_{cl}$, it may also appear that $k^2 - \tilde{\beta}^2 = 0$ in Eq. (13). However, because V is arbitrary, $k^2 - \tilde{\beta}^2$ is a finite constant which is one of a set of constants determined from Eq. (13). Consider the mathematically equivalent problem of $y^2 - x^2 = c^2$ in the limit $x \rightarrow \infty$, where c is independent of x . Then $y \rightarrow x$ while $y^2 - x^2 = c^2$. As a final remark, the modal fields of $n_{co} = n_{cl}$ step profile waveguides with circular symmetry are often called LP or uniformly polarized modes.^{5,6}

We next show how the solutions of the scalar wave equation $\tilde{\mathbf{e}}$ and $\tilde{\beta}$ can be used to construct accurate representation of \mathbf{e} and β , which are themselves solutions of the vector wave equation, Eq. (2).

C. Modes on the $n_{co} \simeq n_{cl} \simeq n$ waveguide: $n_{co} \simeq n_{cl}$ modes

The significant consequence of having n_{co} different from n_{cl} is that the waveguide has polarization properties. The polarization properties are contained within the $\nabla_t \epsilon$ term of the wave equation. The modes of such a waveguide must exhibit these properties and therefore they must be solutions of the vector wave equation. However, since the term $\nabla_t (\mathbf{e}_t \cdot \nabla_t \ln \epsilon)$ is zero when $n_{co} = n_{cl}$, it must have a small,¹² but nevertheless a very important effect for $n_{co} \simeq n_{cl}$. The modes of the $n_{co} \simeq n_{cl}$ waveguide can then be approximated by linear combinations of the modal fields $\tilde{\mathbf{e}}$ of the $n_{co} = n_{cl}$ waveguide. The proper linear combinations are dictated by the symmetries of the waveguide which are fully contained within the $\nabla_t \epsilon$ term of the vector wave equation. The method of constructing the linear combination is simple and is discussed in Sec. III.

Because $\beta \simeq k$ on the $n_{co} \simeq n_{cl}$ waveguide, the transverse fields obey the approximate relationship

$$\mathbf{h}_t \simeq (\epsilon/\mu)^{1/2} \hat{\mathbf{z}} \times \mathbf{e}_t. \quad (14)$$

The longitudinal fields are then found from Maxwell's divergence equations, leading to

$$h_z = (i/\beta) \nabla_t \cdot \mathbf{h}_t, \quad (15)$$

$$e_z = (i/\beta) \{\nabla_t \cdot \mathbf{e}_t + (\nabla_t \ln \epsilon) \cdot \mathbf{e}_t\}, \quad (16a)$$

$$\simeq (i/\beta) \nabla_t \cdot \mathbf{e}_t. \quad (16b)$$

Equation (16b) is sufficiently accurate for our purposes.¹² When $n_{co} \simeq n_{cl}$ we know that $\rho\beta \gg 1$ so that Eqs. (14)–(16) show that the modes of an $n_{co} \simeq n_{cl}$ waveguide are nearly TEM waves.

The propagation constant β for the $n_{co} \simeq n_{cl}$ modes nearly equals $\tilde{\beta}$ determined from Eq. (13). To include small polarization effects one uses a standard method presented in Appendix A, leading to

$$\beta - \tilde{\beta} \simeq \frac{\beta^2 - \tilde{\beta}^2}{2k} = \frac{\int_{A_{co}} \tilde{\mathbf{e}}_t \cdot \nabla_t (\mathbf{e}_t \cdot \nabla_t \ln \epsilon) dA}{2k \int_{A_{co}} \tilde{\mathbf{e}}_t \cdot \mathbf{e}_t dA}, \quad (17)$$

where $k = 2\pi n/\lambda$, $\tilde{\beta}$ and $\tilde{\mathbf{e}}_t$ are defined by Eqs. (12) and (13),

and \mathbf{e}_t and β are defined by Eq. (2). A_∞ is the infinite cross section. Once \mathbf{e}_t is approximated by a linear combination of $\bar{\mathbf{e}}$ fields, Eq. (17) is used to calculate β , where $\bar{\mathbf{e}}_t$ in Eq. (17) is any one of the $\bar{\mathbf{e}}$'s used to approximate \mathbf{e}_t . For a step-index profile Eq. (17) is simplified by using a result of Appendix A,

$$\int_{A_\infty} \bar{\mathbf{e}}_t \cdot \nabla_t (\mathbf{e}_t \cdot \nabla_t \ln \epsilon) dA = \theta_c^2 \oint_{\text{core}} (\nabla_t \cdot \bar{\mathbf{e}}_t) (\mathbf{e}_t \cdot \hat{\mathbf{n}}) dl \quad (18a)$$

$$= i\theta_c^2 \bar{\beta} \oint_{\text{core}} (\bar{\mathbf{e}}_z \cdot \hat{\mathbf{z}}) (\mathbf{e}_t \cdot \hat{\mathbf{n}}) dl, \quad (18b)$$

where \oint_{core} is a line integral around the core-cladding interface, and $\hat{\mathbf{n}}$ is the outward normal to that interface. The small correction to $\bar{\beta}$ obtained from Eq. (17) is necessary to separate the erroneous degenerate $\bar{\beta}$'s found by solving the scalar wave equation rather than the vector wave equation. For example, Eq. (17) includes the small polarization-dependent effects necessary to distinguish the β of a TM from a TE wave.

In summary, the modal fields of the $n_{co} \cong n_{cl}$ waveguide are nearly TEM waves obeying Eqs. (14)–(16), with corrected propagation constants obtained from Eq. (17). The transverse fields are synthesized from linear combinations of the $n_{co} = n_{cl}$ fields defined by Eqs. (12) and (13).

III. CONSTRUCTION OF VECTOR MODAL FIELDS USING THE $n_{co} \cong n_{cl}$ METHOD

We now discuss the problem of constructing approximations of the vector modal fields by linearly combining $n_{co} = n_{cl}$ fields. While it is possible to provide a general mathematical prescription for forming the linear combinations, e.g., see Appendix A, in this section we follow a physically intuitive argument. The philosophy of the method is based on the fact that modal fields must satisfy the symmetry properties of the waveguide. These symmetry properties are contained within the $\nabla_t \epsilon$ term of the vector wave equation and therefore they are automatically included in solutions of this equation. However, it is often possible to guess the appropriate symmetry conditions without solving the vector wave equation. We next provide some examples beginning with circularly symmetric waveguides and then waveguides with two preferred axes of symmetry.

A. Waveguides with circular symmetry

The $n_{co} = n_{cl}$ modes are given by Eq. (12) in terms of the scalar function ψ . By virtue of the circular symmetry, there are in general two solutions of the scalar wave Eq. (13) for each allowed value of $\bar{\beta}$. One solution, ψ_e , has even symmetry while the other, ψ_o , has odd symmetry:

$$\psi_e(r, \phi) = f_l(r) \cos l\phi, \quad \psi_o(r, \phi) = f_l(r) \sin l\phi. \quad (19)$$

In Eq. (19), ϕ is the azimuthal angle and $f_l(r)$ is a solution of

$$\left(\frac{d^2}{dr^2} + \frac{1}{r} \frac{d}{dr} + k^2(r) - \bar{\beta}^2 - \frac{l^2}{r^2} \right) f_l(r) = 0. \quad (20)$$

Thus the $n_{co} = n_{cl}$ waveguide of Sec. II A has four modes for each allowed value of $\bar{\beta}$, i.e.,

$$\bar{\mathbf{e}}_{xe} = f_l(r) \cos(l\phi) \hat{\mathbf{x}}, \quad \bar{\mathbf{e}}_{xo} = f_l(r) \sin(l\phi) \hat{\mathbf{x}}, \quad (21a)$$

$$\bar{\mathbf{e}}_{ye} = f_l(r) \cos(l\phi) \hat{\mathbf{y}}, \quad \bar{\mathbf{e}}_{yo} = f_l(r) \sin(l\phi) \hat{\mathbf{y}}. \quad (21b)$$

We now discuss how to linearly combine these $\bar{\mathbf{e}}$ modal fields to form approximate modal fields of the $n_{co} \cong n_{cl}$ waveguide.

1. The fundamental ($l = 0$) modes

When $l = 0$, there are only two $n_{co} = n_{cl}$ modes, $\bar{\mathbf{e}}_{xe}$ and $\bar{\mathbf{e}}_{ye}$. These fields exist at all frequencies and depend only on r . By virtue of the circular symmetry any linear combination of these two fields must be a modal field of the $n_{co} \cong n_{cl}$ waveguide. Also, from circular symmetry, the $n_{co} \cong n_{cl}$ waveguide has two fundamental modes with equal β 's [as can be verified from Eq. (17)]. We can take one mode to be polarized in the x direction (\mathbf{e}_x) and the other to be polarized in the y direction (\mathbf{e}_y):

$$\mathbf{e}_x = f_0(r) \hat{\mathbf{x}}, \quad \mathbf{e}_y = f_0(r) \hat{\mathbf{y}}, \quad (22)$$

where $f_0(r)$ is the solution of Eq. (20) with $l = 0$.

The two fundamental modes of the circular symmetric $n_{co} \cong n_{cl}$ waveguide are exceptional in that they are the same as the fundamental modes on the $n_{co} = n_{cl}$ waveguide, i.e., they are uniformly polarized throughout the cross section and have the same β 's.

2. Higher-order modes (i.e., $l \geq 1$)

We showed at the beginning of this section that the circularly symmetric waveguide has four $n_{co} = n_{cl}$ modes when $l \neq 0$. Unlike the fundamental modes, none of the $n_{co} = n_{cl}$ fields for $l \geq 1$ are individually modal fields of the $n_{co} \cong n_{cl}$ waveguide. This can be proved¹³ from symmetry considerations together with Eq. (17). Thus we require linear combinations of $\bar{\mathbf{e}}_{xe}$, $\bar{\mathbf{e}}_{xo}$, $\bar{\mathbf{e}}_{ye}$, and $\bar{\mathbf{e}}_{yo}$ to form the higher-order modes.

To form the correct linear combinations, we combine those modes which have the same properties under a rotation by 90° and under reflections in the x and y axes. [It may help at this point to consider a specific example, say the $l = 1$ modes shown in Fig. 2(a).] Thus $\bar{\mathbf{e}}_{xe}$ is combined with $\bar{\mathbf{e}}_{yo}$ because

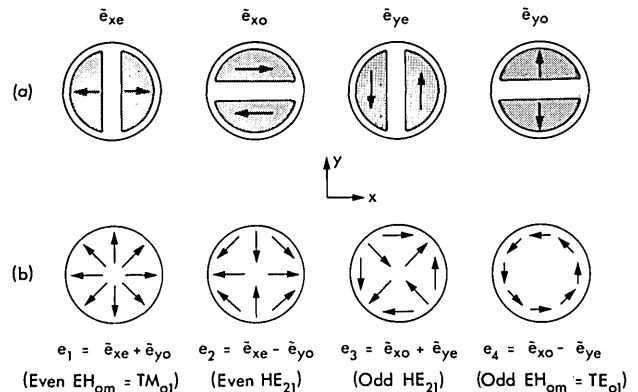


FIG. 2. (a) The $n_{co} = n_{cl}$ or LP modes for $l = 1$. Note that $\bar{\mathbf{e}}_{xe}$ and $\bar{\mathbf{e}}_{yo}$ are symmetric under reflections in the x and y axes, while $\bar{\mathbf{e}}_{xo}$ and $\bar{\mathbf{e}}_{ye}$ are antisymmetric. If any one of the above fields is rotated through an arbitrary angle it transforms into a linear combination of all four. Note also that apart from normalization, $\bar{\mathbf{e}}_{xe} = \mathbf{e}_1 + \mathbf{e}_2$, $\bar{\mathbf{e}}_{xo} = \mathbf{e}_3 - \mathbf{e}_4$, $\bar{\mathbf{e}}_{ye} = \mathbf{e}_3 + \mathbf{e}_4$ and $\bar{\mathbf{e}}_{yo} = \mathbf{e}_1 - \mathbf{e}_2$, where the \mathbf{e} 's are shown in (b). (b) The $n_{co} \cong n_{cl}$ modes for $l = 1$. Under an arbitrary reflection and rotation, \mathbf{e}_1 and \mathbf{e}_4 are unchanged, while either \mathbf{e}_2 or \mathbf{e}_4 transform into linear combinations of \mathbf{e}_2 and \mathbf{e}_4 .

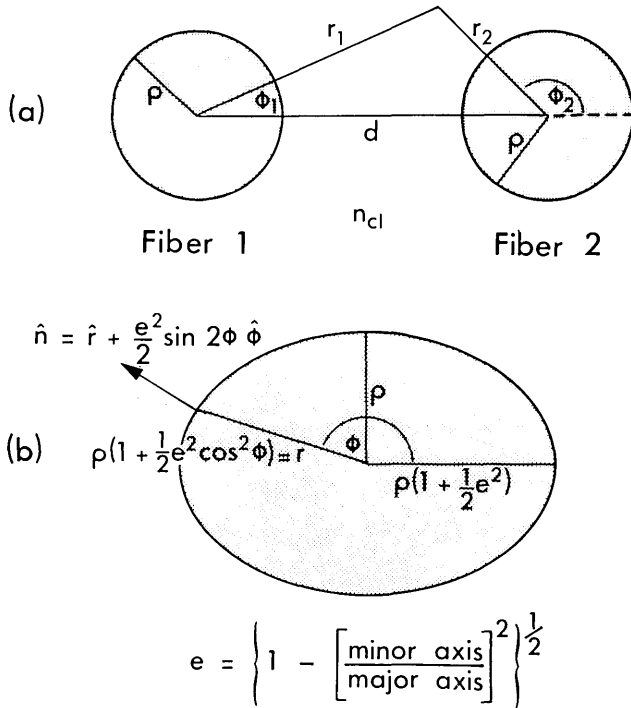


FIG. 3. Waveguides with preferred axes of symmetry. (a) Composite, two-parallel-waveguide system, and (b) an elliptical core.

one rotates into the other, while $\tilde{\mathbf{e}}_{x_0}$ is combined with $\tilde{\mathbf{e}}_{y_0}$ because one rotates into minus the other. Taking symmetric and antisymmetric combinations leads to the 4 modes of the $n_{co} \cong n_{cl}$ waveguide:

$$\mathbf{e}_{t1} = \tilde{\mathbf{e}}_{x_e} + \tilde{\mathbf{e}}_{y_0}, \quad \mathbf{e}_{t2} = \tilde{\mathbf{e}}_{x_e} - \tilde{\mathbf{e}}_{y_0}, \quad (23a)$$

$$\mathbf{e}_{t3} = \tilde{\mathbf{e}}_{x_0} + \tilde{\mathbf{e}}_{y_e}, \quad \mathbf{e}_{t4} = \tilde{\mathbf{e}}_{x_0} - \tilde{\mathbf{e}}_{y_e}, \quad (23b)$$

Using conventional nomenclature,^{14,15} modes 1–4 refer to the even $\text{EH}_{l-1,m}$, even $\text{HE}_{l+1,m}$, odd $\text{HE}_{l+1,m}$, and odd $\text{EH}_{l-1,m}$ modes, respectively. Figure 2(b) illustrates the modes for $l = 1$. These combinations can be shown¹⁶ to be consistent with the symmetry properties of the waveguide. By placing \mathbf{e}_{t1} in Eq. (17) for \mathbf{e}_t and $\tilde{\mathbf{e}}_{x_e}$ for $\tilde{\mathbf{e}}_t$ we obtain β for mode 1 and similarly for the other three modes. In general, the β 's of the EH and HE modes differ from one another. This difference gives rise to a beat phenomenon causing a rotation of the $n_{co} = n_{cl}$ or LP patterns as the mode advances. The stability of the LP mode patterns is set by the difference $|\beta_{HE} - \beta_{EH}|$ in the propagation constants of the two different mode types that form an LP pattern. When $\beta_{HE} = \beta_{EH}$, the $n_{co} = n_{cl}$ modes are also modes of the $n_{co} \cong n_{cl}$ waveguide.

B. Waveguides with two preferred axes of symmetry

Many structures of practical interest have a pair of preferred orthogonal axes of symmetry, e.g., the ellipse and the composite two cylinder waveguide of Fig. 3. When $n_{co} \cong n_{cl}$, the modes of these waveguides can be formed by linear combinations of the $n_{co} = n_{cl}$ modal fields. We now show how to form these combinations, beginning with the fundamental modes.

1. Fundamental modes

It is intuitive that the fundamental modes, those modes

which propagate for all values of frequency, have electric fields that are polarized along one of these two axes of symmetry. Thus the $n_{co} = n_{cl}$ modal fields are the proper approximations of the fundamental fields of the $n_{co} \cong n_{cl}$ waveguide provided the $\hat{\mathbf{x}}$ and $\hat{\mathbf{y}}$ directions of Eq. (12) are aligned with the direction of the symmetry axes. Therefore the fundamental mode has vector fields of the form

$$\mathbf{E}_x = \mathbf{e}_x e^{i\beta x z} = \psi e^{i\beta x z} \hat{\mathbf{x}}, \quad (24a)$$

$$\mathbf{E}_y = \mathbf{e}_y e^{i\beta y z} = \psi e^{i\beta y z} \hat{\mathbf{y}}, \quad (24b)$$

where ψ is the fundamental solution of the scalar wave equation, Eq. (13). The modal propagation constant β_x is found by substituting $\mathbf{e}_t = \tilde{\mathbf{e}}_t = \mathbf{e}_x$ into Eq. (17), while β_y is found by substituting $\mathbf{e}_t = \tilde{\mathbf{e}}_t = \mathbf{e}_y$ into Eq. (17). We have now fully specified the general characteristics of the fundamental modes on waveguides with a pair of preferred orthogonal symmetry axes. The details depend on knowing the solution to the scalar equation. It is apparent that the transmission properties of such waveguides, when propagating only the fundamental modes, are similar to those of anisotropic crystals in that the waveguide has a pair of optical axes.¹⁷

2. Higher-order modes on waveguides with preferred axes of symmetry

In general, the fields of higher-order modes of structures with two preferred axes of symmetry are more complicated than the fundamental modes. In order to appreciate this complication we begin by considering the ellipse. It is clear that for a sufficiently large eccentricity the field of any particular $n_{co} \cong n_{cl}$ mode is represented by Eq. (24), so that the only difference between it and a fundamental mode is in the values of ψ and β . However, it is equally clear that for a sufficiently small eccentricity, this same mode resembles a modal field of a circularly symmetric waveguide, with $\hat{\mathbf{x}}$ and $\hat{\mathbf{y}}$ parallel to the symmetry axes of the ellipse. This transition is sketched in Fig. 4. We can associate each ellipse mode with the fields of a distorted circle mode. For example, the ellipse mode that corresponds to distorting either \mathbf{e}_{t1} or \mathbf{e}_{t2} of Fig. 2 is formed by a linear combination of $\tilde{\mathbf{e}}_{x_e}$ and $\tilde{\mathbf{e}}_{y_0}$, where these $\tilde{\mathbf{e}}$'s are now solutions to the scalar wave equation in elliptical geometry. Consequently, the fields of the ellipse modes \mathbf{e}_{t1} and \mathbf{e}_{t2} are

$$\mathbf{e}_{t1} = a_i \psi_e \hat{\mathbf{x}} + b_i \psi_o \hat{\mathbf{y}} = a_i \tilde{\mathbf{e}}_{x_e} + b_i \tilde{\mathbf{e}}_{y_0}, \quad (25)$$

where $i = 1$ or 2 , ψ_e and ψ_o are solutions of the scalar wave equation in elliptical geometry and are analogous to ψ_e and ψ_o given by Eq. (19) for the scalar wave equation in circular cylindrical geometry. Figure 5 provides an example of ψ_e and ψ_o . The propagation constants associated with ψ_e and ψ_o are denoted $\tilde{\beta}_e$ and $\tilde{\beta}_o$, respectively. These $\tilde{\beta}$'s are different; the difference increases as eccentricity increases.

A heuristic argument can be used for determining the minimum eccentricity necessary for the $l \geq 1$ ellipse modes to be uniformly polarized, i.e., to have the form given by Eq. (24). Anticipating that only a slight eccentricity is necessary, the fields of the ellipse can be approximated by linear combinations of the circle $n_{co} = n_{cl}$ fields $\tilde{\mathbf{e}}_{x_e}$ and $\tilde{\mathbf{e}}_{y_0}$ as far as the present discussion is concerned. Thus uniformly polarized ellipse modes are nearly the $n_{co} = n_{cl}$ or LP modes of the circle. We now recall our discussion of Sec. III B 2 in which we stated that the rate that LP modes rotate into one another depends

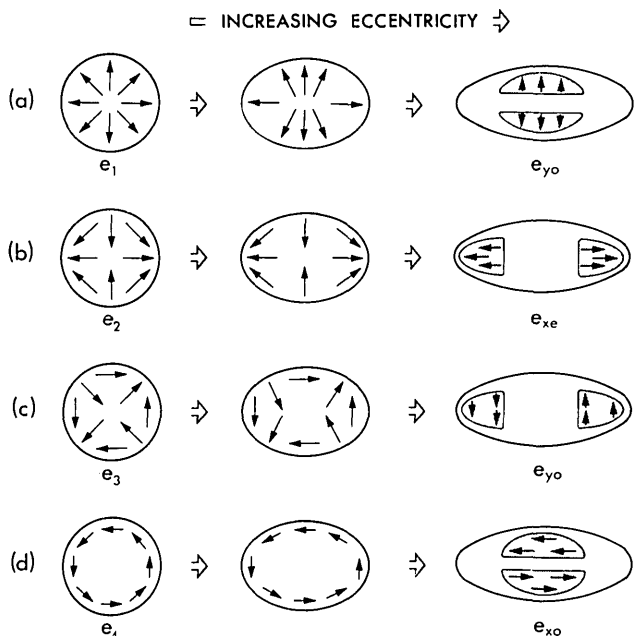


FIG. 4. Transition from circle to ellipse modes for $l = 1$ modes. An electric field vector maintains its orientation to the interface, i.e., if it was initially perpendicular it remains perpendicular, as the eccentricity increases. Using this heuristic principle one can anticipate the way in which a particular circle mode changes as the eccentricity increases.

upon $|\beta_{EH} - \beta_{HE}|$, where β_{EH}, β_{HE} are the β 's of the circular waveguide. When this difference is zero the LP modes are stable, i.e., they are proper modes of the $n_{co} \cong n_{cl}$ waveguide. The stability of circle modes on an ellipse depends upon $\tilde{\beta}_e - \tilde{\beta}_o$, as implied in the preceding paragraph, where $\tilde{\beta}_e, \tilde{\beta}_o$ are the β 's for the ellipse determined from the scalar wave equation. Consequently, the parameter Λ is influential in determining the limiting behavior of ellipse fields, where

$$\Lambda = (\tilde{\beta}_e - \tilde{\beta}_o) / (\beta_{EH} - \beta_{HE}), \quad (26)$$

$\beta_{EH} = \beta_1$ and $\beta_{HE} = \beta_2$ for the particular ellipse modes e_{t1} and e_{t2} given by Eq. (25). When $|\Lambda| \gg 1$, the fields of the ellipse are uniformly polarized. When $|\Lambda| \ll 1$, the ellipse modal fields are the fields of modes on a circularly symmetric waveguide.

The argument given above is tantamount to determining the limiting behavior of a_i/b_i of Eq. (25). It is elementary to find an exact expression for this ratio as a consequence of finding β for ellipse modes. The β associated with the ellipse vector modal field Eq. (25) is found by substituting e_{t1} in Eq. (17) for e_t and substituting either \tilde{e}_{xe} or \tilde{e}_{yo} in Eq. (17) for \tilde{e}_t . The fact that we have two expressions for the same β gives us two equations which, when taken together, determine the ratio a_i/b_i of Eq. (25) in addition to β_i . The algebra is left to Appendix A. For small eccentricity,

$$a_i/b_i = \Lambda \pm (\Lambda^2 + 1)^{1/2} \quad (27)$$

$$\beta_i^2 = [(\tilde{\beta}_e^2 + \tilde{\beta}_o^2)/2] \pm \{[(\tilde{\beta}_e^2 - \tilde{\beta}_o^2)/2]^2 + C^2\}^{1/2}, \quad (28)$$

where $i = 1$ is associated with (+), while $i = 2$ is associated with (-) and $\tilde{\beta}_e, \tilde{\beta}_o$ are from the scalar equation for the ellipse. The parameter C is

$$C = \int_{A_{\infty}} \tilde{e}_{xe} \cdot \nabla_t (\tilde{e}_{yo} \cdot \nabla_t \ln \epsilon) dA / \int_{A_{\infty}} |\tilde{e}_{xe}|^2 dA \quad (29a)$$

$$\cong \beta_1^2 - \beta_2^2 \cong 2k(\beta_1 - \beta_2), \quad (29b)$$

where β_1, β_2 are for circle modes 1 and 2, \tilde{e}_{xe} and \tilde{e}_{yo} are the fields given by Eq. (23) for the circular fiber and $k = 2\pi n/\lambda$. We have used Eq. (17) to deduce Eq. (29b). The parameter Λ is

$$\Lambda = (\tilde{\beta}_e^2 - \tilde{\beta}_o^2)/2C \cong (\tilde{\beta}_e - \tilde{\beta}_o)/(\beta_1 - \beta_2), \quad (30)$$

which is the same as Eq. (26), derived intuitively for small ellipticity. Thus, the composition of a mode depends only on the parameter Λ . When $\Lambda = 0$, the modes are essentially circle modes. When $\Lambda \gg 1$ the modes are nearly uniformly polarized. Equations (27)–(30) are for modes 1 and 2 of the ellipse, when $l \geq 1$. The two other ellipse modes are found analogously.

Identical arguments can be applied to all structures with two preferred axes of symmetry, e.g., the composite two parallel waveguide systems of Fig. 3. Furthermore, the procedure can clearly be generalized to other classes of symmetry.

IV. EXAMPLES: STEP REFRACTIVE INDEX WAVEGUIDES

Sections II and III show how to construct the vector modal fields e, h and their propagation constants β from linear combination of solutions ψ to the scalar wave equation, Eq. (13). Thus when ψ is known the modes are fully specified. We first determine the modes of a step profile waveguide with circular symmetry, since our results can then be compared with the exact forms. Next, we consider a waveguide with an elliptical core and then a composite two parallel cylinder waveguide. These last two examples exhibit several interesting physical properties which our method readily displays.

A. Step-index waveguide with circular symmetry

The radial function $f_l(r)$ for a step profile is found from Eq. (20) and can be written

$$f_l(r) = J_l(\tilde{U}r/\rho) / J_l(\tilde{U}), \quad r \leq \rho \quad (31a)$$

$$f_l(r) = K_l(\tilde{W}r/\rho) / K_l(\tilde{W}), \quad r \geq \rho \quad (31b)$$

where the notation \sim indicates that they are derived from the scalar wave equation, J_l is a Bessel function and K_l is a

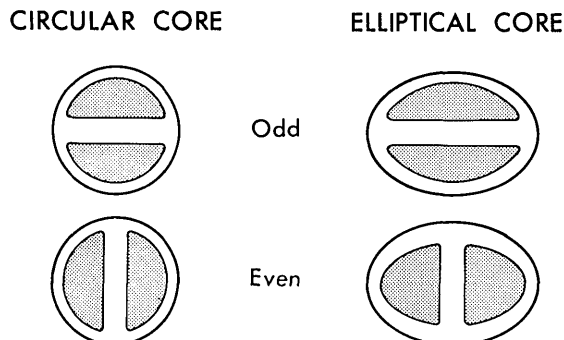


FIG. 5. An example of a solution of the scalar wave equation corresponding to the $l = 1$ mode. The β 's of the even and odd circle mode are identical unlike the β 's for the even and odd modes of the elliptical core.

TABLE I. Modal parameters for a step profile, circularly symmetric waveguide when $n_{co} \cong n_{cl}$.

	Mode 1 Even $\text{EH}_{l-1,m}$ (even $\text{EH}_{0,m} = \text{TM}_{0,m}$)	Mode 2 Even $\text{HE}_{l+1,m}$	Mode 3 Odd $\text{HE}_{l+1,m}$	Mode 4 Odd $\text{EH}_{l-1,m}$ (odd $\text{EH}_{0,m} = \text{TE}_{0,m}$)
Transverse fields \mathbf{e}_t $f_l(r) = \begin{cases} J_l(\tilde{U}r/\rho)/J_l(\tilde{U}), & r \leq \rho \\ K_l(\tilde{W}r/\rho)/K_l(\tilde{W}r/\rho), & r \geq \rho \end{cases}$	$\mathbf{e}_{t1} = \tilde{\mathbf{e}}_{ex} + \tilde{\mathbf{e}}_{oy}$ $= \{\tilde{x} \cos l\phi + \tilde{y} \sin l\phi\}f_l(r)$	$\mathbf{e}_{t2} = \tilde{\mathbf{e}}_{ex} - \tilde{\mathbf{e}}_{oy}$ $= \{\tilde{x} \cos l\phi - \tilde{y} \sin l\phi\}f_l(r)$	$\mathbf{e}_{t3} = \tilde{\mathbf{e}}_{ox} + \tilde{\mathbf{e}}_{ey}$ $= \{\tilde{x} \sin l\phi + \tilde{y} \cos l\phi\}f_l(r)$	$\mathbf{e}_{t4} = \tilde{\mathbf{e}}_{ox} - \tilde{\mathbf{e}}_{ey}$ $= \{\tilde{x} \sin l\phi + \tilde{y} \cos l\phi\}f_l(r)$
Longitudinal fields \mathbf{e}_z $e_z = -i\rho\theta_c(\nabla_t \cdot \mathbf{e}_t)/V$ $g_l^\pm(r) = \begin{cases} \tilde{U}J_{l\pm 1}(\tilde{U}r/\rho)/J_l(\tilde{U}), & r < \rho \\ \tilde{W}K_{l\pm 1}(\tilde{W}r/\rho)/K_l(\tilde{W}), & r > \rho \end{cases}$	$(i/V)\theta_c g_l^-(r) \cos(l-1)\phi$	$-(i/V)\theta_c g_l^+(r) \cos(l+1)\phi$	$-(i/V)\theta_c g_l^+(r) \sin(l+1)\phi$	$(i/V)\theta_c g_l^-(r) \sin(l-1)\phi$
Propagation constants β $\beta - \tilde{\beta} = \frac{\rho\theta_c \int_{A_{in}} \tilde{\mathbf{e}}_t \cdot \nabla_t(\mathbf{e}_t \cdot \nabla_t \ln \epsilon) dA}{2V \int_{A_{in}} \tilde{\mathbf{e}}_t \cdot \mathbf{e}_t dA}$ $\tilde{\beta}^2 = k_{co}^2 - \tilde{U}^2/\rho^2$	$\beta_1 - \tilde{\beta} = -\frac{\theta_c^2 \tilde{U}^2 \tilde{W} K_1(\tilde{W})}{\rho V^3 K_2(\tilde{W})}$ ($l=1$) $\beta_1 - \tilde{\beta} = -\frac{\theta_c^2 \tilde{U}^2 \tilde{W} K_l(\tilde{W})}{2\rho V^3 K_{l+1}(\tilde{W})}$ ($l \neq 1$)	$\beta_2 - \tilde{\beta} = \beta_3 - \tilde{\beta} = -\frac{\theta_c^2 \tilde{U}^2 K_l(\tilde{W})}{2\rho V^3 K_{l-1}(\tilde{W})}$		$\beta_4 - \tilde{\beta} = 0$ ($l=1$) $\beta_4 - \tilde{\beta} = -\frac{\theta_c^2 \tilde{U}^2 \tilde{W} K_l(\tilde{W})}{2\rho V^3 K_{l+1}(\tilde{W})}$ ($l \neq 1$)

modified Hankel function. Note that $l=0$ is for the fundamental mode, $l=1$ for the second mode, and so on. The requirement that $f_l(r)$ and $df_l(r)/dr$ be continuous at $r=\rho$ gives the eigenvalue equation

$$\tilde{U}J_{l+1}(\tilde{U})K_l(\tilde{W}) = \tilde{W}K_{l+1}(\tilde{W})J_l(\tilde{U}), \quad (32)$$

after using the recursion relations for Bessel functions, where \tilde{U} and \tilde{W} are related to the dimensionless parameter V defined by Eq. (7) as

$$V^2 = \tilde{U}^2 + \tilde{W}^2. \quad (33)$$

The propagation constant $\tilde{\beta}$ is defined

$$(\rho\tilde{\beta})^2 = (\rho k_{co})^2 - \tilde{U}^2 = (\rho k_{cl})^2 + \tilde{W}^2, \quad (34)$$

where k_{co} and k_{cl} are defined in relation to Eq. (5). The vector modal fields can then be formed as discussed in Sec. III and are listed in Table I. The propagation constants β are found by substituting the expressions for \mathbf{e}_t in Table I into Eq. (17) for \mathbf{e}_t and substituting either of the two $\tilde{\mathbf{e}}$ fields used to form \mathbf{e}_t into Eq. (17) for $\tilde{\mathbf{e}}_t$. The details are presented in Appendix C with results listed in Table I. Our present approach streamlines the original derivation¹ and in addition provides a simple analytic expression for improving $\tilde{\beta}$ by accounting for the $\nabla_t \epsilon$ term in the vector wave equation. Discarding terms of order θ_c^2 from the exact expression for \mathbf{e}_t leads to the results of Table I, while discarding terms of order θ_c^3 leads to \mathbf{e}_z . The expressions for U ignore θ_c^5 terms. We emphasize that because the step profile is the most rapidly varying $\epsilon(x,y)$ possible, it is therefore the profile most sensitive to polarization effects, i.e., most sensitive to the influence of the $\nabla_t \epsilon$ term in the vector wave equation. Thus the step profile provides a stringent test of the $n_{co} \cong n_{cl}$ method. When the profile is graded, the theoretical procedure for finding modes follows that for the step profile.

1. Stability of LP modes

The $n_{co} = n_{cl}$ or LP modes are not modes of an $n_{co} \neq n_{cl}$ waveguide. The reason is that each LP mode is formed by

combining two proper modes, an $\text{HE}_{l+1,m}$ and $\text{EH}_{l-1,m}$ mode, and these proper modes have different propagation constants, β_{HE} and β_{EH} . Because of the beat phenomenon, when $\beta_{\text{HE}} - \beta_{\text{EH}} \neq 0$, the modes appear¹⁸ to rotate or fade into each other, e.g., $\tilde{\mathbf{e}}_{xe}$ of Fig. 2 after propagating a distance $\pi/|\beta_2 - \beta_1|$, which equals half the beat length, appears like $\tilde{\mathbf{e}}_{yo}$ of Fig. 2. The greater $|\beta_{\text{HE}} - \beta_{\text{EH}}|$, the shorter the beat length and hence the more rapidly the LP modes fade into one another. Using the results of Table I and recursion relations for the K_l functions leads to expressions for the difference in β 's: For $l=1$ modes

$$\beta_1 - \beta_2 = \frac{\theta_c^3}{2\rho} \left(\frac{\tilde{U}^2}{V^3} \right) \frac{K_1^2(\tilde{W})}{K_0(\tilde{W})K_2(\tilde{W})} \left\{ 2 - \frac{\tilde{W}K_0(\tilde{W})}{K_1(\tilde{W})} \right\}. \quad (35)$$

The differences $\beta_4 - \beta_3$ for $l=1$ is found from Eq. (35) by replacing $(-)$ in the $\{\}$ quantity by $(+)$. For $l \geq 2$,

$$\beta_1 - \beta_2 = l \frac{\theta_c^3}{\rho} \left(\frac{\tilde{U}^2}{V^3} \right) \frac{K_l^2(\tilde{W})}{K_{l-1}(\tilde{W})K_{l+1}(\tilde{W})}, \quad (36)$$

which also equals $\beta_3 - \beta_4$. The results for $l=1$ are shown in Fig. 6. Note the special characteristic that at $V \cong 3.8$ the $\tilde{\mathbf{e}}_{xe}$ and $\tilde{\mathbf{e}}_{yo}$ patterns of Fig. 2(a), i.e., the $n_{co} = n_{cl}$ or LP modes, are true modes of the $n_{co} \neq n_{cl}$ waveguide, since at this frequency $\beta_1 = \beta_2$. In contrast, $\beta_4 - \beta_3 \cong 0.25\theta_c^3/\rho$ at $V \cong 3.8$ corresponding to a half beat length $(\pi\rho/0.25\theta_c^3) \cong 1.3 \times 10^4 \rho$ for a typical value of $\theta_c = 0.1$. Thus near $V \cong 3.8$, the mode patterns $\tilde{\mathbf{e}}_{xe}$ and $\tilde{\mathbf{e}}_{yo}$ should appear stable compared to the other two patterns of Fig. 2(a). When $V \gg 1$, $|\beta_1 - \beta_2| \cong |\beta_3 - \beta_4| \cong \theta_c^3 \tilde{U}^2 / 2\rho V^2$.

From Eq. (36), we learn that the β 's are never equal for $l \geq 2$, so that these LP modes are never modes of the circularly symmetric waveguide. Furthermore, the greater l , the greater $|\beta_1 - \beta_2|$ which approximately equals $\theta_c^3 \tilde{U}^2 / 2\rho V^3$ for $l \gg 1$. Consequently, for fixed V , the greater l , the less stable the LP modes. Knowledge of the stability of LP modes is useful when considering waveguides with two preferred symmetry axes. It is also useful for a critical determination of V as well as a sensitive indicator of asymmetries.

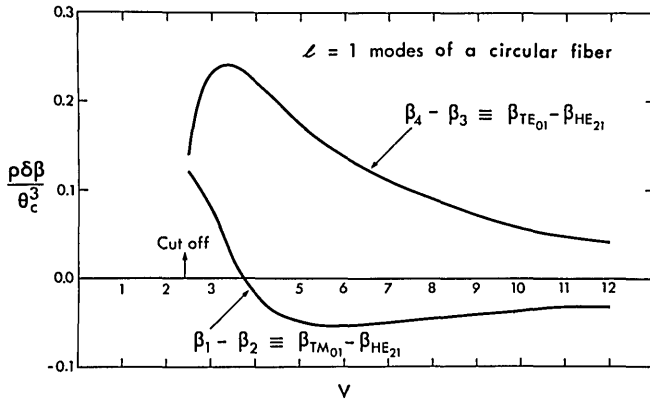


FIG. 6. The difference in β 's for $l = 1$ modes of the circularly symmetric, step profile waveguide. Each LP mode of Fig 2(a) is formed by linear combination of β_1, β_2 modes or β_3, β_4 modes.

B. Step-index ellipse

We showed in Fig. 4 that a slight elliptical deviation from circular symmetry leads to new modes which appear¹⁸ like the uniformly polarized (or LP) modes of the $n_{co} = n_{cl}$ circularly symmetric waveguide shown in Fig. 2(a), except that e must be parallel to one of the two symmetry axes. Now it is interesting to determine the minimum amount of eccentricity for the $n_{co} = n_{cl}$ or LP modes of Fig. 2(a) to be good approximation of the proper ellipse modes. On a waveguide with this minimum eccentricity the modes of a circularly symmetric waveguide are unstable, i.e., they couple power among themselves as they propagate, while the $n_{co} = n_{cl}$ or LP modes of the circularly symmetric fiber are stable. We have shown in Sec. III B 2 that the effect of eccentricity depends crucially upon the parameter Λ , where

$$\Lambda = (\tilde{\beta}_e - \tilde{\beta}_o) / (\beta_{EH} - \beta_{HE}), \quad (37)$$

where β_{EH}, β_{HE} are the propagation constants for the two mode types on a waveguide with circular symmetry [Sec. IV A, Eqs. (35) and (36)], while $\tilde{\beta}_e, \tilde{\beta}_o$ are the even and odd propagation constants of the two mode types on an ellipse obtained by solving the scalar wave equation, Eq. (13), in elliptic geometry. When $\Lambda \gg 1$, the fields of the ellipse correspond approximately to the $n_{co} = n_{cl}$ or LP modes, while when $\Lambda \ll 1$ the fields are approximately those of the true modes of a circularly symmetric waveguide.

1. $l = 1$ ellipse modes

We have previously determined $\beta_{EH} - \beta_{HE}$ as stated by Eqs. (35) and (36). Anticipating that only a small eccentricity is necessary for the LP modes of the circle to resemble ellipse modes, we can determine $\tilde{\beta}_e - \tilde{\beta}_o$ from the scalar wave equation in circular geometry using elementary perturbation methods presented in Appendix B and D leading to

$$\tilde{\beta}_e - \tilde{\beta}_o = \frac{(\theta_c e^2 / 4\rho)(\tilde{U}^2 / V) K_1^2(\tilde{W})}{K_0(\tilde{W}) K_2(\tilde{W})}, \quad (38)$$

where \tilde{U} and \tilde{W} are found from Eq. (32). Consequently, the important parameter Λ of Eq. (37) becomes

$$\Lambda = (1/2)(e/\theta_c)^2 V^2 \{2 \pm \tilde{W} K_0(\tilde{W}) / K_1(\tilde{W})\}^{-1}, \quad (39)$$

where the negative sign is for Λ_{TM} , i.e., for $\beta_{EH} - \beta_{HE}$ in Eq.

(37) to be $\beta_{TM} - \beta_{HE}$, while the positive sign applies to Λ_{TE} , i.e., for $\beta_{TE} - \beta_{HE}$. Equation (39) exhibits the sensitivity of Λ to eccentricity e , defined in Fig. 3, and refractive-index difference θ_c , defined by Eq. (8). For fixed V , the smaller θ_c , the less eccentricity is necessary for the LP modes of the circular cylinder to resemble stable modes of the ellipse. Figure 7 provides a graph of $(\theta_c/e)^2 \Lambda$ vs V . Remembering that when $\Lambda \gg 1$, the LP circle modes are the approximate modes of the ellipse, while when $\Lambda \ll 1$ the circle modes are approximate modes of the ellipse; we see that no eccentricity is required for the LP \tilde{e}_{xe} and \tilde{e}_{yo} modes to resemble ellipse modes at $V \cong 3.8$. This is anticipated from Fig. 6, since these LP modes are then true modes of the circular cylinder without any perturbation. Since the minimum value for $\Lambda \cong 2(e/\theta_c)^2$, only a minute eccentricity ($e \geq 2\theta_c$) is required for the LP circle modes to be stable. The higher-order ellipse modes can be determined in a similar fashion. They should appear more like Λ_E than Λ_{TM} , since $\beta_{HE} - \beta_{EH}$ is nonzero as discussed in Sec. IV A.

2. Fundamental or $l = 0$ modes of the ellipse

In Sec. III B 1 we noted that the transmission properties of an elliptical waveguide propagating only the two fundamental modes are similar to those of an anisotropic crystal, i.e., they both have orthogonal optical axes. The anisotropic properties of the waveguide depend upon the difference in propagation constants β_x, β_y of the x and y polarized ellipse modes, respectively, where¹⁹

$$\beta_x - \beta_y = \left(\frac{e^2 \theta_c^3}{8\rho} \right) \left(\frac{\tilde{U}^2 \tilde{W}^2}{V^3} \right) \left\{ 1 + \tilde{U} \frac{K_0^2(\tilde{W}) J_2(\tilde{U})}{K_1^2(\tilde{W}) J_1(\tilde{U})} \right\}, \quad (40)$$

assuming $e^2 \ll 1$, where \tilde{U} and \tilde{W} are found from the solution of Eq. (32) for the fundamental, $l = 0$ or HE_{11} mode. If the fiber is illuminated by linearly polarized light at 45° to the optical or symmetry axes, then both fundamental modes are excited equally and the wave becomes elliptically polarized as it propagates. Because of the beat phenomenon, the E vector appears to rotate. The length for a 360° rotation is $2\pi|\beta_x - \beta_y|^{-1}$. In Fig. 8 we have plotted $\beta_x - \beta_y$ as a function of V .

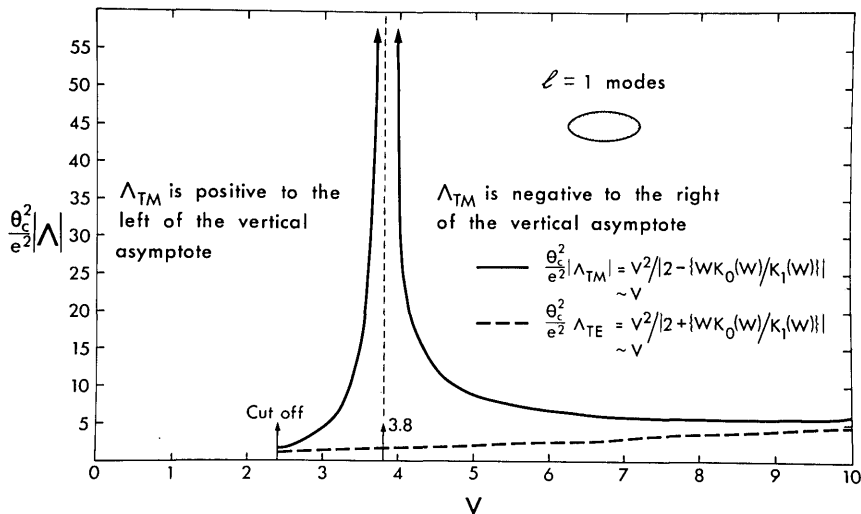
C. Two identical parallel step-index waveguides with circular symmetry

The determination of modes on the composite two waveguide system of Fig. 3 is completely analogous to that of the ellipse as outlined in Sec. III B, except that the scalar solution ψ for the two-cylinder geometry is now required. There is no exact solution for ψ . Instead, ψ is approximated in the usual manner by a symmetric and antisymmetric superposition of the fields of the waveguides in isolation, while $\tilde{\beta}$ is approximated using the same perturbation method on the scalar wave equation as with the ellipse. The procedure is discussed in Appendixes B and E, where all of the following results are derived.

1. Fundamental modes

There are four fundamental modes as shown in Fig. 9, each with a different β and each having e_t parallel to one of the two axes of symmetry. It is well known^{14,20} that under the appropriate excitation conditions, identical parallel waveguides interchange all power between each other in length $l = \pi/(\beta_+ - \beta_-)$, where l is half the beat length, β_+, β_- are the propaga-

FIG. 7. The parameter Λ defined by Eq. (39) determines the ratio a_i/b_i of the ellipse $l = 1$ fields, Eq. (25). When $|\Lambda| \gg 1$, the modes are uniformly polarized (LP modes), while when $|\Lambda| \ll 1$ the modal fields are those of a circular core.



tion constants of the symmetric and antisymmetric modes, respectively, and $\beta_+ - \beta_- \cong \tilde{\beta}_+ - \tilde{\beta}_-$, where

$$\tilde{\beta}_+ - \tilde{\beta}_- = \frac{2\theta_c \tilde{U}^2 K_0(\tilde{W}d/\rho)}{\rho V^3 K_1^2(\tilde{W})} \quad (41)$$

for either x - or y -polarized modes, d is the center-to-center separation, and \tilde{U} , \tilde{W} are found from Eq. (32). This result agrees with that found²⁰ from Maxwell's equation when $\theta_c \ll 1$. Since the $\tilde{\beta}$'s are solutions of the scalar wave equation, the power transfer between parallel cylinders is essentially a scalar phenomenon. However, like the ellipse, unless \mathbf{e}_t is parallel to one of the symmetry axes, it appears to rotate as the field propagates along the cylinders. The length required for an apparent 180° rotation is $\pi/(\beta_x - \beta_y)$ when \mathbf{E} is initially 45° to the symmetry axes, where

$$\beta_x - \beta_y = \frac{\theta_c^3 \tilde{U}^2 K_0(\tilde{W}d/\rho)}{\rho V^3 K_1^2(\tilde{W})} [1 - 2I_1(\tilde{W})K_1(\tilde{W})] \quad (42)$$

for either symmetric or antisymmetric modes, where $I_1(\tilde{W})$ is a modified Bessel function. It is interesting to determine the amount α° in degrees that \mathbf{E} rotates in the length necessary for total power transfer between the cylinder. This is given by 180° times the ratio

$$\frac{\beta_x - \beta_y}{\tilde{\beta}_+ - \tilde{\beta}_-} = \frac{1}{2} \theta_c^2 [1 - 2I_1(\tilde{W})K_1(\tilde{W})] \sim \frac{\theta_c^2}{2} \left(1 - \frac{1}{V}\right). \quad (43)$$

Thus the angular rotation is less than $\alpha^\circ = \theta_c^2 (90^\circ)$, i.e., less than about 1° in a length required for total power transfer for a typical fiber with $\theta_c = 0.1$.

2. $l = 1$ modes

There are in general 8 mode types on the two cylinder waveguide, i.e., an even and an odd mode for each of the configurations shown in Fig. 9. The dependence of higher-order modes on the center-to-center separation distance d is directly analogous to the dependence of the ellipse modes on eccentricity. When the fibers are sufficiently close, the modes of the two-cylinder system are well approximated by fields of the $n_{co} = n_{cl}$ fiber, i.e., the LP modes of each fiber in isolation, but with \mathbf{E} parallel to the axes of symmetry. When the fibers are sufficiently separated, the modes are approximated by the fields of the $n_{co} \cong n_{cl}$ waveguides in isolation but with \mathbf{e}_t again parallel to the symmetry axes. The situation is illustrated in Fig. 11 for one of the $l = 1$ modes of the two waveguide system.

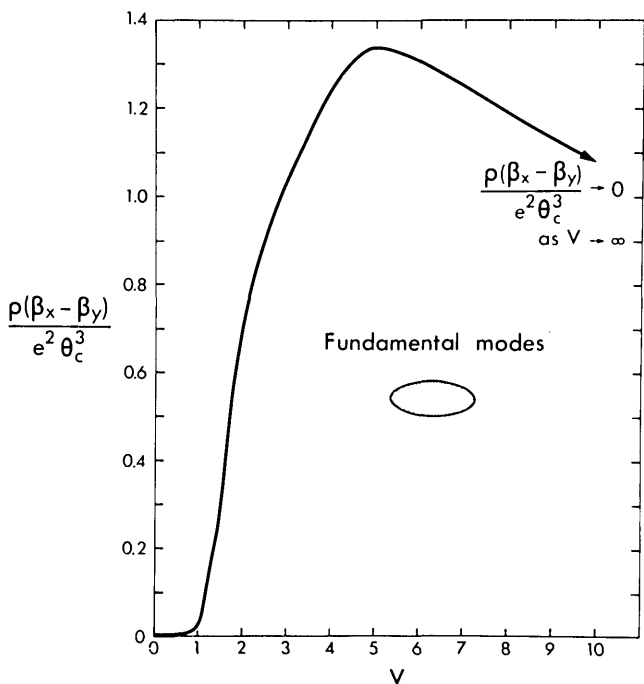


FIG. 8. The difference in β 's of the x - and y -polarized, fundamental ellipse modes.

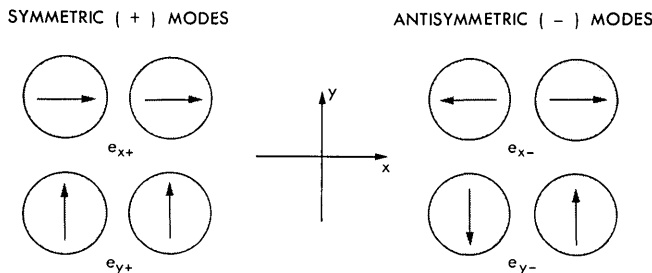


FIG. 9. The four fundamental modes of the two-parallel-waveguide system shown in Fig. 3(a).

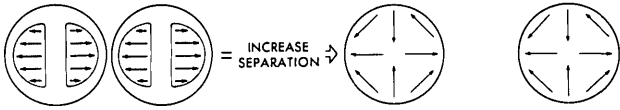


FIG. 10. The transition of an $l = 1$ mode of the two-parallel-waveguide system as the separation increases. When the fibers are close, the composite mode appears like a superposition of two \tilde{e}_{x_0} modes of Fig. 2(a). When the fibers are well separated, the composite mode appears like a superposition of the e_2 model of Fig. 2(b).

In other words, large eccentricity in the ellipse is analogous to small separation between the two cylinders. The modes of the two waveguide system are formed by a linear combination of the same modes as for the ellipse. Accordingly, the logic of Sec. III B 2 applies directly so that the parameter Λ is again important in establishing the limiting behavior of the modal fields. As in the ellipse

$$\Lambda = (\tilde{\beta}_e - \tilde{\beta}_o) / (\beta_{EH} - \beta_{HE}), \quad (44)$$

where $\beta_{EH} - \beta_{HE}$ are given by Eqs. (35) and (36) and $\tilde{\beta}_e - \tilde{\beta}_o$ is the difference between the scalar β 's of an even and odd mode, both symmetric on antisymmetric. From Appendix B and E,

$$\tilde{\beta}_e - \tilde{\beta}_o = \frac{\theta_c \tilde{U}^2}{\rho V^3} \frac{K_2(\tilde{W}d/\rho)}{K_0(\tilde{W})K_2(\tilde{W})}, \quad (45)$$

where \tilde{U} and \tilde{W} are found from Eq. (32). Substituting Eqs. (45) and (35) or (36) into Eq. (44) leads to

$$\Lambda = \frac{2 K_2(\tilde{W}d/\rho)}{\theta_c^2 K_1^2(\tilde{W})} \left(2 \pm \frac{\tilde{W}K_0(\tilde{W})}{K_1(\tilde{W})} \right)^{-1}. \quad (46)$$

The negative sign in Eq. (46) applies for $\beta_{EH} - \beta_{HE} = \beta_{TM} - \beta_{HE}$, which is shown in Fig. 11, while the positive sign is for $\beta_{TE} - \beta_{HE}$. When $\Lambda \gg 1$, the modes of the two-cylinder waveguide are formed by an $n_{co} = n_{cl}$ or LP mode on each of the two cylinders. When $\Lambda \ll 1$, the modes of the two-cylinder waveguide are approximated by a mode of the circularly symmetric waveguide on each of the two cylinders. When the cylinders are well electromagnetically separated, i.e., when $d > 5\rho$ or when $K \gg 1$ the individual cylinders support the modes of a circularly symmetric waveguide in isolation. When the cylinders are strongly coupled, e.g., when $d \cong 2\rho$ or $V \cong 2.4$ ($l = 1$ cutoff V), the LP \tilde{e}_{x_0} or \tilde{e}_{y_0} modes of Fig. 2 are stable on each cylinder. When $V \cong 3.8$, we have already learned from Fig. 6 that these LP modes are proper modes of the individual cylinders. The other Λ is not shown but we know that it lacks the singularity at $V \cong 3.8$ as predicted from Fig. 6.

V. DISCUSSION

Our objective was to approximate the vector fields and their propagation constants for modes of those optical waveguides with $n_{co} \cong n_{cl}$. The transverse vector fields are synthesized from simple linear combinations of solutions to the scalar wave equation. The ∇_ϵ terms of the vector wave equation set the correct linear combinations and separate erroneous degeneracies introduced by solving only the scalar wave equation. We account for this effect using the symmetry of the waveguide cross section and an elementary perturbation method.

An important property of circularly symmetric waveguides with $n_{co} \cong n_{cl}$ is that the slightest asymmetry causes dramatic changes in the form of the modal fields. When the asymmetry has a preferred axis, the $n_{co} = n_{cl}$ or LP modes become stable, i.e., they become the approximate modes of the deformed structure.

Although the perturbation theory of this paper requires only that $n_{co} \cong n_{cl}$, we have nevertheless used an example of small eccentricity to illustrate the mechanics of the method without resorting to special functions. This problem can also be solved using a perturbation method in which the only small parameter is eccentricity, assuming the fields of the circularly symmetric waveguide are known exactly.

Cautionary note on using LP modes as the modes for circularly symmetric waveguides. Many authors have used $n_{co} = n_{cl}$ or LP modes as if they were the proper modes of circularly symmetric waveguides. In general, however, the intensity pattern and the plane of polarization of the LP modes rotates as the mode propagates. Consequently, investigations (e.g., by coupled-mode theory) of those loss and coupling mechanisms that lack circular symmetry are subject to error when using LP modes. This problem does not arise using the proper $n_{co} \cong n_{cl}$ modes derived here and elsewhere.¹ In other words, the fields of a perturbed waveguide need be represented by a complete set of the proper modes of the unperturbed waveguide and not by the LP pseudo-modes. However, as we pointed out above, there are highly specialized

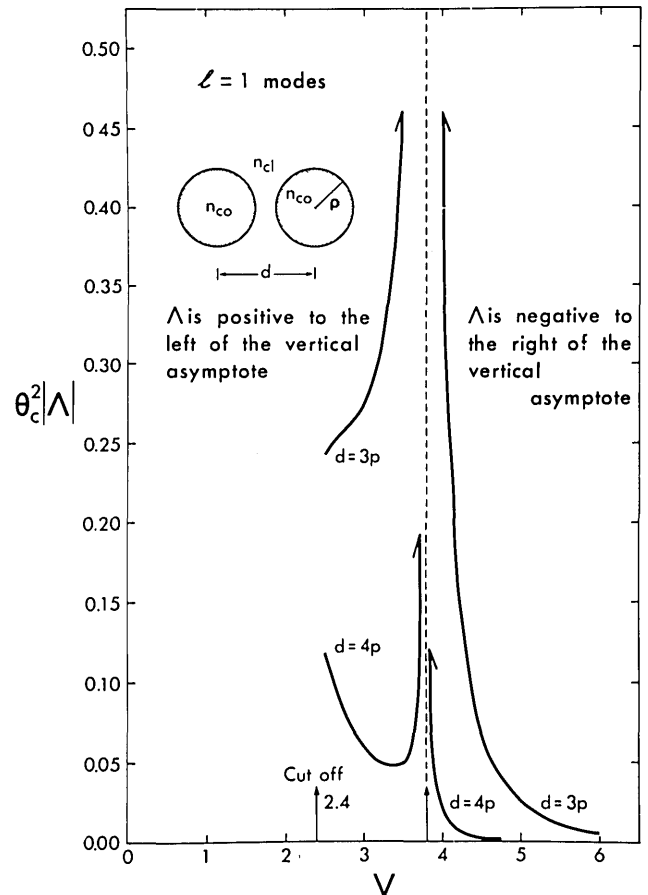


FIG. 11. The parameter Λ defined by Eq. (4b) which determines the composition of $l = 1$ modes.

perturbations for which the fields of LP modes, *properly oriented with respect to the symmetry axes of the deformation*, are a good approximation to the modes of the perturbed structure. On multimoded waveguides the inaccuracies of LP modes are smoothed out, but such problems are better suited to a ray analysis.⁹

ACKNOWLEDGMENTS

We thank Dr. J. D. Love and Dr. C. Pask for their helpful comments.

APPENDIX A. MATHEMATICAL DETAILS OF THE $n_{co} \cong n_{cl}$ METHOD

β Correction Formula

The fundamental result of the $n_{co} \cong n_{cl}$ method, Eq. (17), is proved by a deviation of the method used to obtain modal orthogonality. The exact field \mathbf{e}_t satisfies

$$[\nabla_t^2 + (k^2 - \beta^2)]\mathbf{e}_t = -\nabla_t(\mathbf{e}_t \cdot \nabla_t \ln \epsilon), \quad (A1)$$

while an $n_{co} \cong n_{cl}$ field satisfies

$$[\nabla_t + (k^2 - \tilde{\beta}^2)]\tilde{\mathbf{e}}_t = 0. \quad (A2)$$

Dot product Eq. (A1) with $\tilde{\mathbf{e}}_t$ and Eq. (A2) with \mathbf{e}_t , subtract the two equations, and then integrate over the infinite cross section A_∞ . The term

$$\int_{A_\infty} (\tilde{\mathbf{e}}_t \cdot \nabla_t^2 \mathbf{e}_t - \mathbf{e}_t \cdot \nabla_t^2 \tilde{\mathbf{e}}_t) dA$$

is converted to a line integral at infinity using the vector Green's theorem. This term vanishes since \mathbf{e}_t and $\tilde{\mathbf{e}}_t$ decay exponentially. The final result is Eq. (17). No approximations have been made in obtaining the expression for $\beta^2 - \tilde{\beta}^2$. We note, however, that $\beta^2 - \tilde{\beta}^2 \cong 2k(\beta - \tilde{\beta})$, since $\beta \cong \tilde{\beta} \cong k$.

When $\epsilon(x,y)$ is a step function, the numerator in Eq. (17) is simplified by integrating by parts and using the identity

$$(\nabla \ln \epsilon) dA = [\ln(\epsilon_{cl}/\epsilon_{co})]\delta(B)\hat{\mathbf{n}} dl = -\theta_c^2 \delta(B)\hat{\mathbf{n}} dl, \quad (A3)$$

where $\delta(B)$ is a delta function at the boundary of the core, dA is a differential area element with a portion of its perimeter at the boundary, and $\hat{\mathbf{n}}$ is the outward normal to the boundary. We then have

$$\int_{A_\infty} \tilde{\mathbf{e}}_t \cdot \nabla_t(\mathbf{e}_t \cdot \nabla_t \ln \epsilon) dA = \theta_c^2 \oint_B (\nabla_t \cdot \tilde{\mathbf{e}}_t)(\mathbf{e}_t \cdot \hat{\mathbf{n}}) dl. \quad (A4)$$

Vector Modal Fields

We now give the mathematical procedure for forming the vector electric fields \mathbf{e}_t of a waveguide with $n_{co} \cong n_{cl}$. This requires approximating \mathbf{e}_t by a linear combination of the fields $\tilde{\mathbf{e}}$ of all $n_{co} = n_{cl}$ modes with equal or nearly equal β 's. Usually this can be reduced to two modes after applying symmetry arguments. Thus

$$\mathbf{e}_{ti} = a_i \tilde{\mathbf{e}}_a + b_i \tilde{\mathbf{e}}_b, \quad (A5)$$

where $i = 1$ or 2 . In all our examples $\tilde{\mathbf{e}}_a \cdot \tilde{\mathbf{e}}_b = 0$, but in general

$$\int_{A_\infty} \tilde{\mathbf{e}}_a \cdot \tilde{\mathbf{e}}_b dA = 0, \quad (A6)$$

where A_∞ is the infinite cross section. Now we substitute Eq. (A5) into Eq. (17) for \mathbf{e}_t and substitute $\tilde{\mathbf{e}}_a$ into Eq. (17) for $\tilde{\mathbf{e}}_t$. This leads to

$$(C_{aa} + \tilde{\beta}_a^2 - \beta_i^2)a_i + (C_{ab})b_i = 0, \quad (A7)$$

where $\tilde{\beta}_a$ is the β for $\tilde{\mathbf{e}}_a$ and

$$C_{aj} = \frac{\int_{A_\infty} \tilde{\mathbf{e}}_a \cdot \nabla_t(\tilde{\mathbf{e}}_j \cdot \nabla_t \ln \epsilon) dA}{\int_{A_\infty} |\tilde{\mathbf{e}}_a|^2 dA}, \quad (A8)$$

where j is either a or b . We again substitute Eq. (A5) into Eq. (17) but this time substitute $\tilde{\mathbf{e}}_b$ for \mathbf{e}_t . This leads to

$$(C_{ba})a_i + (C_{bb} + \tilde{\beta}_b^2 - \beta_i^2)b_i = 0, \quad (A9)$$

where $\tilde{\beta}_b$ is $\tilde{\beta}$ for $\tilde{\mathbf{e}}_b$ and C_{ba} , C_{bb} are given by Eq. (A8), replacing a by b . Taken together, Eqs. (A8) and (A9) determine β_i and the ratio a_i/b_i . Equating the determinant of the two equations to zero leads to an equation for β_i :

$$(C_{aa} + \tilde{\beta}_a^2 - \beta_i^2)(C_{bb} + \tilde{\beta}_b^2 - \beta_i^2) - C_{ab}C_{ba} = 0, \quad (A10)$$

from which we find that

$$\beta_i^2 = \frac{C_{ab} + \tilde{\beta}_a^2 + C_{bb} + \tilde{\beta}_b^2}{2} \pm \left[\left(\frac{C_{aa} + \tilde{\beta}_a^2 - C_{bb} - \tilde{\beta}_b^2}{2} \right)^2 + C_{ab}C_{ba} \right]^{1/2}, \quad (A11)$$

where β_1 goes with (+) and β_2 with (-). Knowing β_i^2 , we have a_i/b_i from Eq. (A9):

$$a_i/b_i = (\beta_i^2 - \beta_b^2 - C_{bb})/C_{ba}. \quad (A12)$$

No approximations have been made other than Eq. (A5). In many cases $\tilde{\beta}_i^2 \gg C_{jj}$, where j is either a or b and also $\tilde{\beta}_a^2 - \tilde{\beta}_b^2 \gg C_{aa} - C_{bb}$. We also often have that $C_{ba} \cong C_{ab} \cong C$. With these assumptions, we have

$$\beta_i^2 = [(\tilde{\beta}_a^2 + \tilde{\beta}_b^2)/2] \pm C(\Lambda^2 + 1), \quad (A13)$$

$$\Lambda = (\tilde{\beta}_a^2 - \tilde{\beta}_b^2)/2C, \quad (A14)$$

$$a_i/b_i = \Lambda \pm (\Lambda^2 + 1)^{1/2}, \quad (A15)$$

where $C = C_{ab} \cong C_{ba}$ given by Eq. (A8).

APPENDIX B. PERTURBATION METHODS FOR THE SCALAR WAVE EQUATION

β Correction formula

In the text we require an expression for β of the scalar wave equation for a slightly elliptical core and also for two parallel waveguides. The method of derivation follows the philosophy already given in Appendix A. Suppose we have two different scalar wave equations,

$$\{\nabla_t^2 + k^2\}\psi = \tilde{\beta}^2\psi, \quad (B1)$$

$$\{\nabla_t^2 + \bar{k}^2\}\bar{\psi} = \bar{\beta}^2\bar{\psi}. \quad (B2)$$

Multiply Eq. (B1) by $\bar{\psi}$ and Eq. (B2) by ψ and subtract:

$$\{\bar{\psi}\nabla_t^2\psi - \psi\nabla_t^2\bar{\psi}\} + \{k^2 - \bar{k}^2\}\psi\bar{\psi} = \{\bar{\beta}^2 - \tilde{\beta}^2\}\psi\bar{\psi}. \quad (\text{B3})$$

Equation (B3) is now integrated over the infinite cross section. Green's theorem is used to convert the first term to a line integral at infinity, which is zero. The final result is

$$\bar{\beta}^2 - \tilde{\beta}^2 = \frac{\int_{A_\infty} (k^2 - \bar{k}^2)\psi\bar{\psi} dA}{\int_{A_\infty} \psi\bar{\psi} dA}. \quad (\text{B4})$$

The usefulness of Eq. (B4) is that we usually have a good approximation for $\bar{\psi}$ and $k^2 - \bar{k}^2$ is known. In the text we use $\bar{\beta}^2 - \tilde{\beta}^2 \cong 2k(\bar{\beta} - \beta)$.

Scalar Fields

In the text we approximated ψ by cylindrical functions for the ellipse with small ellipticity, and $\bar{\psi}$ for the two-cylinder waveguide was approximated using $\bar{\psi} = \bar{\psi}_1 \pm \bar{\psi}_2$, where $\bar{\psi}_1, \bar{\psi}_2$ are the scalar solutions of the two waveguides in isolation. Thus it is unnecessary to present the formal derivations of these elementary approximations. However, in certain cases, e.g., such as two waveguides that differ slightly, it is useful to have the results of the formal approach. The method again parallels that of Appendix A. We approximate ψ_i by

$$\psi_i = a_i\bar{\psi}_a + b_i\bar{\psi}_b, \quad (\text{B5})$$

where $\bar{\psi}_a$ and $\bar{\psi}_b$ do not obey $\int_{A_\infty} \bar{\psi}_a\bar{\psi}_b dA = 0$ for the two-parallel-waveguides system, since $\bar{\psi}_a$ and $\bar{\psi}_b$ are solutions of *different* scalar wave equations. Now we substitute Eq. (B5) into Eq. (B4) in precisely the same way as described in Appendix A, leading to

$$(C_{aa} + \bar{\beta}_a^2 - \beta_i^2)a_i + [C_{ab} + D_a(\bar{\beta}_a^2 - \beta_i^2)]b_i = 0, \quad (\text{B6a})$$

$$\beta^2 = \tilde{\beta}^2 + \frac{\theta_c^2 \int_0^{2\pi} d\phi [f'_l(\rho) \cos(l-1)\phi \cos l\phi \cos\phi + \{lf_l(\rho)/\rho\} \cos(l-1)\phi \sin l\phi \sin\phi]}{\int_{A_\infty} f_l^2(r) \cos^2 l\phi dA}, \quad (\text{C3a})$$

$$= \tilde{\beta}^2 - \left(\frac{\theta_c}{\rho}\right)^2 \left(\frac{\tilde{U}}{V}\right)^2 \frac{\tilde{W}K_l(\tilde{W})}{K_{l+1}(\tilde{W})}, \quad l \neq 1 \quad (\text{C3b})$$

$$= \tilde{\beta}^2 - 2 \left(\frac{\theta_c}{\rho}\right)^2 \left(\frac{\tilde{U}}{V}\right)^2 \frac{\tilde{W}K_1(\tilde{W})}{K_2(\tilde{W})}, \quad l = 1 \quad (\text{C3c})$$

where standard Bessel function recurrence relations and the eigenvalue equation, Eq. (32) have been employed. The corrections to the remaining three β 's are listed in Table I.

APPENDIX D. MATHEMATICAL DETAILS FOR THE ELLIPTICAL CORE WAVEGUIDE

Here we provide some intermediate steps leading to the expression $\tilde{\beta}_e - \tilde{\beta}_o$ for the elliptical core waveguide presented in the text. The perturbation formula Eq. (B4) gives $\tilde{\beta}$ in terms of $\bar{\beta}$ and $\bar{\psi}$. Since it is assumed that the ellipticity is very slight, we take these barred quantities to be the solutions of the scalar wave equation for a circular cylinder and assume $\bar{\psi} \cong \psi$. The ellipse departs only slightly from the circular geometry within a crescent-shaped region about the x axis of

$$[C_{ba} + D_b(\bar{\beta}_b^2 - \beta_i^2)]a_i + (C_{bb} + \bar{\beta}_b^2 - \beta_i^2)b_i = 0, \quad (\text{B6b})$$

where

$$C_{pq} = \frac{\int_{A_\infty} (k^2 - \bar{k}^2)\bar{\psi}_p\bar{\psi}_q dA}{\int_{A_\infty} \bar{\psi}_p^2 dA}, \quad (\text{B7})$$

$$D_j = \frac{\int_{A_\infty} \bar{\psi}_a\bar{\psi}_b dA}{\int_{A_\infty} \bar{\psi}_j^2 dA}, \quad (\text{B8})$$

where p, q , and i can equal either a or b . The D_j term is nonzero when $\bar{\psi}_a$ and $\bar{\psi}_b$ are not orthogonal but is usually small and can be neglected. The results for β_i and a_i/b_i are then given by Eqs. (A11) and (A12) or Eqs. (A13)–(A15).

APPENDIX C. CORRECTION OF $\tilde{\beta}$ FOR THE STEP-INDEX FIBER WITH CIRCULAR SYMMETRY

Once the linear combinations in Eqs. (23) are known, Eq. (17) is used to calculate the correction to $\tilde{\beta}$ produced by the $\nabla_t \epsilon$ term. For example, consider the linear combination

$$\mathbf{e}_{t1} = \bar{\mathbf{e}}_{xe} + \bar{\mathbf{e}}_{y0} \quad (\text{C1a})$$

$$= (\cos l\phi \hat{x} + \sin l\phi \hat{y})f_l(r) \quad (\text{C1b})$$

$$= (\cos(l-1)\phi \hat{r} + \sin(l-1)\phi \hat{\phi})f_l(r). \quad (\text{C1c})$$

Let $\mathbf{e}_t = \mathbf{e}_{t1}$ and $\bar{\mathbf{e}}_t = \bar{\mathbf{e}}_{xe}$ in Eq. (17). We could also take $\bar{\mathbf{e}}_t = \bar{\mathbf{e}}_{y0}$, the final answer is the same. Using

$$\nabla_t \cdot \bar{\mathbf{e}}_{xe} = f'_l(r) \cos l\phi \cos\phi + [lf_l(r)/r] \sin l\phi \sin\phi \quad (\text{C2})$$

and Eq. (18a), we have

Fig. 3, so that $k^2 - \bar{k}^2 = k_{c1}^2 = (\theta_c k_{co})^2$ in this perturbation region and zero elsewhere. The perturbation exists close to the ellipse boundary so that $\psi(r, \phi) \cong \psi(\rho, \phi)$ in the region of integration of Eq. (B4), with $dA = (1/2)(e\rho)^2 \cos^2\phi d\phi$. Now substituting $\psi_e = f_1(r) \cos\phi$, which is the $l = 1$ solution of Eq. (20), into Eq. (B4) leads to

$$\tilde{\beta}_e^2 - \tilde{\beta}^2 = \frac{3}{4} \left(\frac{e}{\rho}\right)^2 \frac{\tilde{U}^2 K_1^2(\tilde{W})}{K_2(\tilde{W})K_0(\tilde{W})}. \quad (\text{D1})$$

Substituting $\psi_o = f_1(r) \cos\phi$ into Eq. (B4) leads to

$$\tilde{\beta}_o^2 - \tilde{\beta}^2 = (\tilde{\beta}_e^2 - \tilde{\beta}^2)/3. \quad (\text{D2})$$

The difference between these two equations leads to the expressions in the text noting that $\tilde{\beta}_e^2 - \tilde{\beta}_o^2 \cong 2k(\tilde{\beta}_e - \tilde{\beta}_o)$.

APPENDIX E. MATHEMATICAL DETAILS FOR THE COMPOSITE TWO-CYLINDER WAVEGUIDE

Here we provide some intermediate steps leading to the expression for $\beta_+ - \beta_-$ for the two-cylindrical waveguide system. The perturbation formula Eq. (B4) is again used, this time with the barred quantities representing the solution to one of the waveguides in isolation and the perturbation region the core of the other. We then approximate ψ by $\psi_{\pm} = \bar{\psi}_1 \pm \bar{\psi}_2$ and $\bar{\psi} = \psi$ in Eq. (B4). Neglecting terms $\int_{\text{core } 2} \bar{\psi}_1^2 dA$ and $\int_{A_{\infty}} \bar{\psi}_1 \bar{\psi}_2 dA$ leads to

$$\bar{\beta}_{\pm}^2 = \bar{\beta}^2 \pm (\theta_c k_{co})^2 \int_{\text{core } 2} \bar{\psi}_1 \bar{\psi}_2 dA / \int_{A_{\infty}} \bar{\psi}_1^2 dA. \quad (\text{E1})$$

These integrals are evaluated by the Bessel function addition formulas. $\beta_{\pm e}$ and $\beta_{\pm o}$ are found by placing ψ_{1e} and ψ_{1o} in Eq. (E1).

The correction to $\bar{\beta}_{\pm}$ for finite $\nabla_t \epsilon$ terms is found by substituting the ellipse fields into Eq. (17), leading to

$$\beta_{x+}^2 = \bar{\beta}_+^2 + \phi_c^2 \oint \psi_+(\nabla \psi_+ \cdot \hat{\mathbf{x}})(\hat{\mathbf{n}} \cdot \hat{\mathbf{x}}) dl / \int_{A_{\infty}} \psi_+^2 dA \quad (\text{E2})$$

for \mathbf{e}_{x+} of the fundamental mode, as an example, where \oint is a line integral over both fibers. Neglecting terms whose integrand contains two exponentially decaying functions leads to

$$\beta_{x+}^2 = \bar{\beta}^2 + 2 \left(\oint \hat{\mathbf{n}} \cdot \hat{\mathbf{x}} [\bar{\psi}_1 (\nabla_t \bar{\psi}_1 \cdot \hat{\mathbf{x}}) + \bar{\psi}_2 (\nabla_t \bar{\psi}_1 \cdot \hat{\mathbf{x}}) + \psi_1 (\nabla_t \bar{\psi}_2 \cdot \hat{\mathbf{x}})] dl \right). \quad (\text{E3})$$

These integrals are evaluated using

$$K_0 \frac{\bar{W}r_1}{\rho} = \sum_{l=-\infty}^{\infty} (-1)^l \cos l \phi_2 I_l \frac{\bar{W}r_2}{\rho} K_l \frac{\bar{W}d}{\rho}, \quad (\text{E4})$$

where r_1 , r_2 , and ϕ_2 are shown in Fig. 3.

¹A. W. Snyder, "Asymptotic expressions for eigenfunctions and eigenvalues of dielectric or optical waveguides," *IEEE Trans. MTT* **17**, 1130-1138 (1969).

²R. Yamada and Y. Inabe, "Guided waves in an optical square-law medium," *J. Opt. Soc. Am.* **64**, 964-969 (1974).

³J. Okoshi and K. Okamoto, "Analysis of wave propagation in inhomogeneous optical fibers using a variational method," *IEEE Trans. MTT* **22**, 938-945 (1974).

⁴C. N. Kurtz, "Scalar and vector mode relations in gradient-index light guides," *J. Opt. Soc. Am.* **65**, 1235-1240 (1975). This paper is specialized to waveguides of circular symmetry. Then standard perturbation methods can be applied to the vector wave equation, with the vector operator ∇_t^2 expanded in circular coordinates. Solutions to the $\nabla_t \epsilon = 0$ portion of the equation automatically obey the appropriate symmetry properties of the structure because they are built into ∇_t^2 . The $\nabla_t \epsilon = 0$ portion of the vector wave equation can then be reduced to a cylindrical scalar wave equation.

⁵D. Gloge, "Weakly guiding fibers," *Appl. Opt.* **10**, 2252-2258 (1971).

⁶A. W. Snyder and C. Pask, "Light absorption in the bee photoreceptor," *J. Opt. Soc. Am.* **68**, 998-1008 (1972).

⁷P. M. Morse and H. Feshbach, *Methods of Theoretical Physics*, Part I (McGraw-Hill, New York, 1953), p. 116.

⁸R. B. Adler, "Waves on inhomogeneous cylindrical structures," *Proc. IRE* **40**, 339-348 (1952).

⁹A. W. Snyder and J. D. Love, *Optical waveguide theory* [Wiley and Chapman and Hall, London (in press)].

¹⁰Recall that the potential of an electrostatic dipole can be expressed by two independent parameters, the dipole moment $p = Qd$ and the separation distance d between a plus and minus charge, each of strength Q . If d is sufficiently small, then the potential ϕ at an arbitrary position is $\phi(p, d) \simeq \phi(p, o)$ where $\phi(p, o)$ is the potential of a point ($d = o$) dipole. A point dipole is unphysical because (a) charges that occupy the same position cancel and (b) p is arbitrary because $Q = \infty$. Nevertheless, the fields of a physical ($d \neq o$) dipole are well approximated by those of the point dipole. Note that p , d , and Q of the dipole play the roles of V , θ_c and λ^{-1} , respectively, of the waveguide.

¹¹L. D. Landau and E. M. Lifshitz, *Electrodynamics of Continuous Media* (Pergamon, New York, 1963), p. 285.

¹²It may appear that the $\nabla_t \ln \epsilon$ has a large effect for rapidly varying ϵ profiles; however, this term is bounded by θ_c^2 . Taking the extreme situation of a step profile, where $\epsilon = \epsilon_{co} + (\epsilon_{cl} - \epsilon_{co})s(r - \rho)$ and $s(r - \rho)$ is a step function, we see that $\nabla_t \ln \epsilon = \theta_c^2 \delta(r - \rho)$. In other words, $\nabla_t \ln \epsilon$ is zero except at $r = \rho$, but the delta function $\delta(r - \rho)$ has a minute strength of θ_c^2 , where θ_c is given by Eq. (8). While it is true that the $\nabla_t \ln \epsilon$ term is most significant for step profiles, it is usually incorporated into the mathematics via the boundary conditions. We show that our procedure leads to highly accurate results even for this extreme case (Sec. IV).

¹³A circularly symmetric waveguide is unchanged if it is rotated through an arbitrary angle or reflected in an axis. Hence if a mode of the waveguide is rotated through an arbitrary angle it must remain a mode (not necessarily the same mode) with the same β . Now, if the pattern $\bar{\mathbf{e}}_{x_e}$ of Fig. 2(a), for example, is rotated through an arbitrary angle it is then represented by a linear combination of all four patterns in Fig. 2(a). Thus if the individual patterns are modes of the waveguide, all four must have the same β . But if the fields $\bar{\mathbf{e}}_{x_e}$, $\bar{\mathbf{e}}_{x_o}$, $\bar{\mathbf{e}}_{y_o}$ are substituted into Eq. (17) we find that the four corrected β 's are not all equal. Therefore $n_{co} = n_{cl}$ modes are not $n_{co} \cong n_{cl}$ modes.

¹⁴N. S. Kapany and J. J. Burke, *Optical Waveguides* (Academic, New York, 1972).

¹⁵D. Marcuse, *Light Transmission Optics* (Van Nostrand Reinhold, Princeton, 1972).

¹⁶The patterns \mathbf{e}_1 and \mathbf{e}_4 of Fig. 2(b) are unchanged by reflection in an arbitrary axis and by rotation through an arbitrary angle, consistent with their being nondegenerate modes of a circularly symmetric waveguide. However, under arbitrary rotation and reflections \mathbf{e}_2 changes into a pattern which is a linear combination of \mathbf{e}_2 and \mathbf{e}_3 . Symmetry demands that this new combination is also a mode, which in turn requires that \mathbf{e}_2 and \mathbf{e}_3 have identical β 's. Indeed, by substituting \mathbf{e}_2 and \mathbf{e}_3 into Eq. (17) we verify that they have identical β 's. Thus the linear combinations given by Eq. (23) are consistent with the requirements of symmetry and the results of Eq. (17). Analogous arguments show that these consistencies remain when $l \neq 1$.

¹⁷M. Born and E. Wolf, *Principles of Optics*, 3rd edition (Pergamon, New York, 1964).

¹⁸E. Snitzer and H. Osterberg, "Observed dielectric waveguide modes in the visual spectrum," *J. Opt. Soc. Am.* **51**, 499-505 (1961).

¹⁹This result is found by substituting the fields $\bar{\mathbf{e}}_x = \psi \hat{\mathbf{x}}$ and $\bar{\mathbf{e}}_y = \psi \hat{\mathbf{y}}$ into Eq. (17) to determine β_x and β_y , where ψ is the solution to the scalar wave equation in elliptical geometry. It is not sufficient to approximate ψ by the solutions of the circular symmetric fiber as done for $\bar{\beta}_e - \bar{\beta}_o$ in Appendix D. Instead, higher-order terms are necessary. Alternatively,⁹ one can perturb about Maxwell's equations in circular symmetry as formulated in Ref. 21; however, because \mathbf{e}_l must include terms of order θ_c^2 , the previously reported result of Marcuse (Ref. 22) is inaccurate. We have included θ_c^2 terms using the expansion presented in Ref. 1.

²⁰A. W. Snyder, "Coupled mode theory for optical fibers," *J. Opt. Soc. Am.* **62**, 1268-1277 (1972). Note that the coupling coefficient is $C = (\bar{\beta}_+ - \bar{\beta}_-)/2$, where C is given by Eq. (26a) of the 1972 paper.

²¹A. W. Snyder, "Mode propagation in optical waveguides," *Electron. Lett.* **6**, 561-562 (1970).

²²D. Marcuse, *Theory of Dielectric Optical Waveguides* (Academic, New York, 1974), pp. 159, 164.